Cellular Physiology and Biochemistry

Cell Physiol Biochem 2012;30:778-790
DOI: 10.1159/000341457
Published online: August 02, 2012
Accepted: June 26, 2012

1015-8987/12/0303-0778$38.00/0

Original Paper

Furanodiene, a Natural Product, Inhibits Breast Cancer Growth Both *in vitro* and *in vivo*

Zhangfeng Zhong[a*] Yuanye Dang[a*] Xia Yuan[b] Wei Guo[b] Yingbo Li[a] Wen Tan[a] Jingrong Cui[b] Jinjian Lu[a] Qingwen Zhang[a] Xiuping Chen[a] Yitao Wang[a]

[a]State Key Laboratory of Quality Research in Chinese Medicine, Institute of Chinese Medical Sciences, University of Macau, Macau, China; [b]State Key Laboratory of Natural and Biomimetic Drugs, School of Pharmaceutical Sciences, Peking University, Beijing, China; *Co-first author

Key Words
Furanodiene • Breast cancer • Proliferation •Cell cycle • Apoptosis

Abstract
Purpose: Previous studies have reported that the *Curcuma wenyujin* Y.H. Chen et C. Ling extract, which has a high furanodiene content, showed anti-cancer effects in breast cancer cells *in vitro*. The present study was designed to evaluate the *in vitro* and *in vivo* anti-cancer activity of furanodiene. ***Methods:*** The *in vitro* effects of furanodiene were examined on two human breast cancer cell lines, MCF-7 and MDA-MB-231 cells. Assays of proliferation, LDH release, mitochondrial membrane potential ($\Delta\Psi m$), cell cycle distribution, apoptosis and relevant signaling pathways were performed. The *in vivo* effect was determined with MCF-7 tumor xenograft model in nude mice. ***Results:*** Furanodiene significantly inhibited the proliferation and increased the LDH release in both cell lines in a dose-dependent manner. $\Delta\Psi m$ depolarization, chromatin condensation, and DNA fragmentation were also observed after furanodiene treatment. Furanodiene dose-dependently induced cell cycle arrest at the G0/G1 phase. The protein expressions of *p*-cyclin D1, total cyclin D1, *p*-CDK2, total CDK2, *p*-Rb, total Rb, Bcl-xL, and Akt were significantly inhibited by furanodiene, whereas the protein expressions of Bad and Bax, and the proteolytic cleavage of caspase-9, caspase-7, and poly-ADP-ribose polymerase (PARP) were dramatically increased. Furthermore, the z-VAD-fmk markedly reversed the furanodiene-induced cell cytotoxicity, the proteolytic cleavage of caspase-9, and DNA fragmentation but did not affect the proteolytic cleavage of PARP, whereas the Akt inhibitor VIII increased the furanodiene-induced cytotoxicity and PARP cleavage. In addition, furanodiene dose-dependently suppressed the tumor growth *in vivo*, achieving 32% and 54% inhibition rates after intraperitoneal injection of 15 mg/kg and 30 mg/kg, respectively. ***Conclusions:*** Taken together, we concluded that furanodiene suppresses breast cancer cell growth both *in vitro* and *in vivo* and could be a new lead compound for breast cancer chemotherapy.

Prof. Yi-Tao Wang and Dr. Xiuping Chen
Institute of Chinese Medical Sciences, University of Macau
Av. Padre Tomas Pereira Taipa, Macau (China)
Tel. +853-83974872, E-Mail ytwang@umac.mo, E-Mail xpchen@umac.mo

Introduction

Products made from natural sources have been regarded as a key source of anti-cancer agents in drug discovery and development. Many natural products and their derivatives have been successfully categorized according to the standard repertoire of cancer chemotherapy, such as paclitaxel, vinblastine, and vincristine. In recent years, the anti-cancer potential of natural products from medicinal plants, especially those used in traditional Chinese medicine, have been gradually recognized by the scientific community [1-5]. A few pure compounds isolated from traditional Chinese medicine, such as berberine, curcumin, quercetin, and so on, have been studied to treat cancer both *in vitro* and *in vivo* [6-8].

Curcuma wenyujin Y.H. Chen et C. Ling (*WenYuJin* in Chinese), a widely prescribed traditional Chinese herb in clinical cancer therapy, has been proven to possess anti-cancer properties [9]. Furthermore, the elemene isolated from *C. wenyujin* Y.H. Chen et C. Ling has been approved by the State Food and Drug Administration (SFDA) as a new second-class drug for cancer chemotherapy [10]. A previous study of the authors revealed that furanodiene (Fig. 1A), a sesquiterpene identified more than 40 years ago, is abundant in *C. wenyujin* Y.H. Chen et C. Ling [11]. However, the bioactivity and potential action mechanisms of furanodiene have not been fully investigated. Previous studies have revealed that furanodiene protects mice from D-galactosamine (D-GalN)/LPS, D-GalN/TNFα- induced acute liver injury [12, 13], and suppresses the 12-O-tetradecanoylphorbol- 13-acetate (TPA)-induced inflammation in the ears of mice [14]. Recent studies reported that furanodiene significantly inhibits HL-60, PC3, SGC-7901, and HT-1080 cell proliferation *in vitro* and exhibits inhibitory effects on the growth of uterine cervical (U14) and sarcoma 180 (Sl80) tumors in mice [15]. Furanodiene inhibits the growth of HL-60 leukemia cells by inducing apoptosis through TNFR1-mediated extrinsic apoptotic pathways [16]. Furanodiene was also reported to inhibit HepG2 cell growth by causing cell cycle arrest at G2/M and inducing apoptosis through MAPK signaling and mitochondria-caspase pathways [17]. More recently, we found that furanodiene exhibited a potential anti-angiogenic effect through the suppression of endothelial cell growth, invasion, migration, and tube formation *via* the regulation of the PI3K pathway in human umbilical vein endothelial cells *in vitro* and on zebrafish *in vivo* [18]. A more recent study demonstrated that furanodiene also prevents metastasis of breast cancer through blockage of NF-κB-dependent MMP-9 and VEGF activation [19]. In addition, an ethanol extract of *Curcuma phaeocaulis* Valeton containing furanodienone, germacrone, and furanodiene induced breast cancer cell apoptosis by increasing the reactive oxygen species formation, decreasing $\Delta\Psi m$, regulating Bcl-2 family protein expression, and activating caspases [20]. These data suggested that furanodienone possesses certain anti-cancer effects. However, the data showed low potency to HepG2 cells and the underlying mechanisms remains unclear. Compared with HepG2 cells, the current primary data revealed that the breast cancer cells were more sensitive to furanodiene. Therefore, the anti-cancer effect of furanodiene was investigated, and the potential mechanisms involved were explored in both *in vitro* and *in vivo* models in the present study.

Materials and Methods

Reagents

Furanodiene (>96%) was isolated and identified similarly to a previous report [21]. Doxorubicin (Dox), tamoxifen (TAM), pan-caspase inhibitor (z-VAD-fmk), and Akt inhibitor VIII were obtained from Sigma-Aldrich (St. Louis, MO, USA). The RPMI-1640 culture medium was obtained from Gibco (Maryland, USA). The fetal bovine serum (FBS), phosphate-buffered saline (PBS), penicillin–streptomycin (PS), and 0.25% (w/v) trypsin/1 mM EDTA were purchased from Invitrogen (Carlsbad, CA, USA). The 3-[4,5-dimethyl-2-thiazolyl]-2,5-diphenyltetrazolium bromide (MTT), propidium iodide (PI), and 5,5',6,6'-tetrachloro-1,1',3,3'-tetraethyl-

benzimidazolylcarbocyanine iodide (JC-1) were purchased from Molecular Probes (Eugene, USA). The RIPA lysis buffer was obtained from Santa Cruz (Santa Cruz, USA). The Cytotoxicity Detection Kit (LDH) used was purchased from Roche Diagnostics (Mannheim, Germany) and the DNA extraction kit was obtained from Beyotime (Haimen, China). The primary antibodies against phospho-cyclin D1 (Thr286) (*p*-cyclin D1), phospho-CDK2 (Thr160) (*p*-CDK2), phospho-Rb (Ser795) (*p*-Rb (Ser795)), phospho-Rb (Ser807/811) (*p*-Rb (Ser807/811)), cyclin D1, CDK2, Bcl-2, Bcl-xL, Bax, Bad, Bok, Puma, p53, caspase-9, caspase-7, poly-ADP-ribose polymerase (PARP), phospho-Akt (Ser473) (*p*-Akt), Akt, β-actin, and the secondary antibodies were obtained from Cell Signaling (Danvers, USA).

Cell culture

The MDA-MB-231 and MCF-7 human breast cancer cells, the MCF-10A non-tumorigenic breast epithelial cells, and the HL-7702 normal human hepatocytes were obtained from ATCC (Manassas, USA). MDA-MB-231, MCF-7 and HL-7702 cells were maintained at 37 °C under an atmosphere of 5% CO_2 and 95% air using RPMI-1640 medium supplemented with 10% (v/v) heat-inactivated FBS and antibiotics (100 U/mL penicillin, 100 μg/mL streptomycin). The MCF-7 cells were exposed to TAM without the use of phenol red RPMI-1640 and heat-inactivated FBS. The culture of MCF-10A cells was as our previous report [22].

MTT assay

The anti-proliferative effect of furanodiene on breast cancer cells was performed using an MTT assay as described previously [17]. Briefly, 100 μL samples of exponentially growing MDA-MB-231 cells (1.5×10^4/well) and MCF-7 cells (1.0×10^4/well) were planted in 96-well plates. Cell viability was determined after furanodiene treatment by adding 100 μL MTT (1 mg/mL) for another 4 h. After discarding the supernatant, 100 μL DMSO was added to each well to solubilize the formazan, followed by 10 min agitation in the dark. The absorbance at 570 nm was recorded using a Multilabel counter (Perkin Elmer, Singapore). MTT assay was also performed on MCF-10A (1.0×10^4/well) and HL-7702 cells (1.0×10^4/well) to test the toxic selectivity. Dox was used as positive control. In addition, the general caspases inhibitor z-VAD-fmk and Akt inhibitor VIII were pretreated with cells for 1 h before furanodiene treatment to explore the role of caspases and Akt.

LDH assay

The LDH released from the cells after furanodiene treatment was measured with a commercial detection kit according to a modified version of the manufacturer's protocol. Briefly, 24 h after furanodiene treatment, 70 μL of supernatants (total volume was 100 μL) was transferred to a new 96-well plate. The residual supernatants were removed. The cells were then lysed with 1% Triton-X lysis solution (30 μL/well) for 30 min at 37 °C followed by the addition of 70 μL PBS solution. A total of 50 μL supernatant were taken from each well to react with the LDH substrate. The percentage of LDH release was calculated using the following formula:

%LDH Release = Spontaneous LDH Release/Maximum LDH Release (Supernatants + Lysate Supernatants) × 100%.

JC-1 assay

The JC-1 assay for mitochondrial membrane potential (ΔΨm) was performed according to the previous report [23]. Briefly, the cells were cultured in black 96-well plates (with transparent bottom) as described in the previous report (1.5×10^4/well) and treated with different concentrations of furanodiene for 4 h. The culture medium was removed and the cells were washed with 100 μL PBS per well twice. The cells were then incubated with 100 μL PBS (containing 2.5 μg/mL JC-1 and 10 mM glucose) for 15 min at 37 °C. The Red (*Ex/Em*, 550 nm/600 nm) and green fluorescence (*Ex/Em*, 485 nm/535 nm) were monitored with a Multilabel counter and the ratio of the red fluorescence to green fluorescence was calculated. Furthermore, following the treatment described above, JC-1 fluorescence was also observed via fluorescent microscopy and the images were taken using an Axiovert 200 fluorescent microscope (Carl Zeiss) and AxioCam HRC CCD camera (Carl Zeiss).

Hoechst 33342 staining

The MCF-7 cells were cultured and treated with furanodiene as described above. After fixing with 3.7% paraformaldehyde for 30 min, the cells were stained with Hoechst 33342 (1 μg/mL) for 30 min. The photographs were taken using an Axiovert 200 fluorescent microscope (Carl Zeiss) and AxioCam HRC CCD camera (Carl Zeiss).

Cell cycle and apoptosis assay

Cell cycle distribution after furanodiene treatment was determined according to the previous report [17]. The MCF-7 cells were treated as described above, collected, and washed twice with ice-cold PBS, and harvested by centrifugation at 350 ×*g* for 5 min. The step was then followed by fixing in 1 mL ice-cold 70% ethanol at –20 °C overnight. The cells were retrieved by centrifugation and incubated with 100 μL PI stain solution (20 μg/mL PI, 8 μg/mL RNase) for 30 min in the dark. The cell apoptosis and cell cycle distribution were analyzed using flow cytometry (BD FACSCanto™, BD Biosciences, San Jose, USA) based on the sub-G1 cell population and DNA content. TAM was used as a positive control. The results were analyzed using Mod Fit LT software (version 3.0).

Agarose gel electrophoresis assay

After the 24 h treatment of MCF-7 cells with furanodiene, the cells were collected and the fragmented DNA was isolated using a DNA extraction kit (Beyotime, China) according to the manufacturer's instructions. Equal amounts of DNA were subjected to electrophoresis on a 1 % agarose gel at 90 V for 1 h to observe the appearance of DNA ladder, visualized using a UV light, and then photographed.

Western blotting assay

After the MCF-7 cells were treated in the desired conditions, the cells were harvested, and the total proteins were extracted with RIPA lysis buffer containing 1% PMSF and 1% protease inhibitor cocktail for 30 min. Equal amounts of total protein, as determined using the BCA Protein Assay Kit, were separated by appropriate SDS-PAGE, and then transferred onto a PVDF membrane. After blocking with 5% nonfat dried milk for 1 h, the membrane was incubated with a specific primary antibody (1:1000), followed by incubation with corresponding second antibodies (1:1000) at 37 °C for 1 h. The specific protein bands were visualized using an ECL advanced Western blot detection kit. The densitometric analysis of band intensity was conducted with Quantity One Software (Bio-Rad). The expression levels were normalized with β-actin, and the control level was set at 100%.

Nude mice xenograft studies

All BALB/c nude mice were provided by Vital River Laboratories (Beijing, China). The mice were maintained under specific pathogen-free conditions, provided with sterilized food and water, and housed in positive pressure isolators at 12 h light/dark cycles. The use of animals was approved by the animal review boards of the School of Pharmaceutical Sciences, Peking University, with a confirmation of adherence to the ethical guidelines for the care and use of animals. Human breast cancer MCF-7 xenografts were established by inoculating 2×10^6 cells s.c. into the nude mice. After 15 days, the mice were randomized into control and treated groups and received vehicle, cyclophosphamide (CTX, 30 mg/kg), and furanodiene (15 mg/kg and 30 mg/kg) by intraperitoneal administration once daily for 8 days. The mice were sacrificed on day 9, and the tumors were excised and weighted.

Data analysis

All data represent the mean of three separately performed experiments. Data are presented as mean ± SEM. The significance of intergroup differences was evaluated by one-way analyses of variance using SPSS 11.5 software. Statistical differences were considered significant at $P < 0.05$.

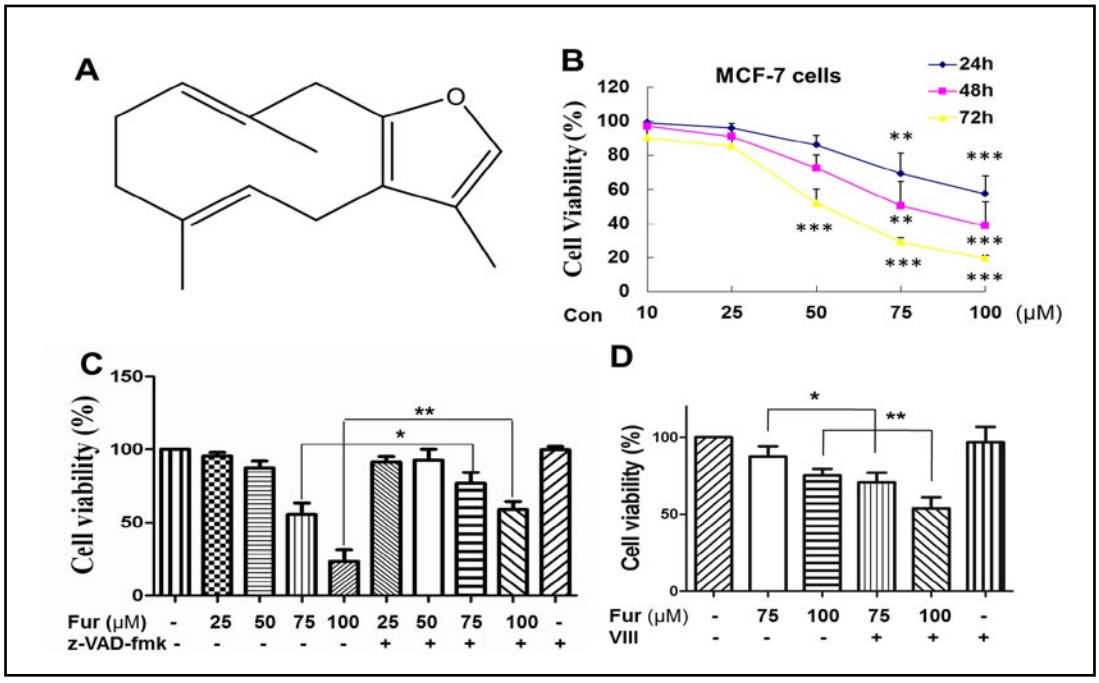

Fig. 1. The chemical structure (A) and the anti-proliferation effect of furanodiene on breast cancer cells (B–D). Cell viability was determined by MTT assay. The MCF-7 cells were treated with different concentrations of furanodiene for 24, 48, and 72 h (B). Effect of z-VAD-fmk (C) and Akt inhibitor VIII (D) on furanodiene-treated MDA-MB-231 cells (C) and MCF-7 cells (D). Con, concentration. Data are expressed as mean ± SEM. In B, $^{**}P < 0.05$, $^{***}P < 0.01$ *vs.* control, respectively; In C and D, $^{*}P < 0.05$, $^{**}P < 0.01$ *vs.* 75 μM and 100 μM furanodiene groups, respectively.

Results

Furanodiene suppresses breast cancer cell proliferation

The anti-proliferative effect of furanodiene was firstly assessed using MDA-MB-231 and MCF-7 cells. As shown in Fig. 1B, furanodiene inhibited the proliferation of MCF-7 cells in a dose- and time-dependent manner, which was also observed in MDA-MB-231 cells (Fig. 1C). The 1 h pretreatment with z-VAD-fmk could significantly reverse the furanodiene-induced anti-proliferation in MDA-MB-231 cells, whereas the Akt inhibitor VIII dramatically enhanced this effect in MCF-7 cells (Fig. 1C and D). Furthermore, furanodiene (0 μM to 100 μM) showed no effect on MCF-10A and HL-7702 cell proliferation after 48 h treatment, whereas Dox significantly inhibited the proliferation of both cell lines at 1 μM and 0.5 μM, respectively (Fig. 2A, B). In addition, compared with the control group, the LDH released from both breast cancer line cells were dramatically increased after 24 h treatment with furanodiene (Fig. 2C). Furthermore, a dose-dependent increase was also observed in both cell lines.

Furanodiene depolarizes ΔΨm in breast cancer cells

Compared with the control group, the JC-1 fluorescence ratio (red/green) was dramatically decreased after 4 h of furanodiene incubation in MDA-MB-231 (Fig. 3A). A total of 100 μM furanodiene induced the MDA-MB-231 ΔΨ*m* decline by 64.49% as calculated by the JC-1 fluorescence ratio. Similar with the microplate reader results, fluorescence microscopy showed intense red fluorescence in intact MCF-7 cells. However, after treatment with 50 μM furanodiene, the red fluorescence significantly decreased, whereas the green fluorescence increased. In groups treated with 100 μM furanodiene (Fig. 3B), only sporadic red fluorescence was observed against the intense green fluorescence, suggesting the significant decrease or

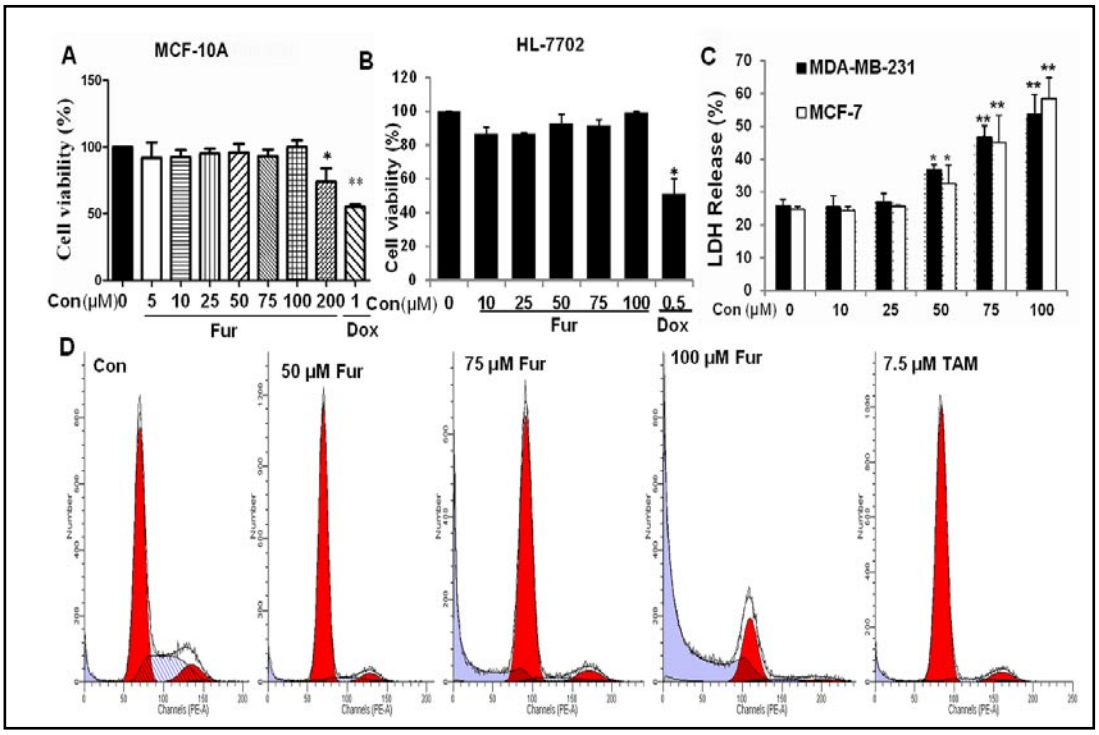

Fig. 2. The cytoxicity of furanodiene (Fur) on non-tumorigenic breast epithelial cells MCF-10A (A), normal liver cells HL-7702 (B), and its effect on LDH release (C) and the cell cycle in breast cancer line cells (D). MCF-10A and HL-7702 cells were treated with various concentrations of furanodiene or Dox for 48 h, respectively. Cell viability was determined with MTT assay. MDA-MB-231 and MCF-7 cells were treated with different concentrations of furanodiene for 24 h, and the LDH release to culture medium was determined. The MCF-7 cells were treated with furanodiene or TAM for 24 h, and the cell cycles were analyzed by flow cytometry. Con, concentration. Data are expressed as mean ± SEM. $^{**}P < 0.05$ *vs.* control and $^{***}P < 0.01$ *vs.* control.

loss of $\Delta\Psi m$. The results show that furanodiene could dose-dependently decrease the $\Delta\Psi m$ of breast cancer cells.

Furanodiene induces G0/G1-phase cell cycle arrest and apoptosis

The flow cytometry assay showed that furanodiene modulated the MCF-7 cell cycle progression by inducing cycle arrest at the G0/G1-phase (Fig. 2D). Compared with untreated cells, the percentage of cells treated with 100 μM furanodiene for 24 h at the G0/G1 phase was increased from 68.12% ± 4.32% to 82.81% ± 7.54%, and the S phase decreased from 22.93% ± 4.54% to 10.37% ± 7.39% (Table 1). Furthermore, furanodiene induced the fractionation of nuclei accumulated at sub-G1 in a dose-dependent manner (Table 1). However, the 24 h treatment with TAM showed no effect on the percentage of cells at sub-G1 (Fig. 2D).

The apoptotic effect of furanodiene was investigated by Hoechst fluorescence staining in MCF-7 cells. Furanodiene caused significant cellular morphological changes at 50 μM for 48 h, including nuclear condensation and the partition of cytoplasm and nucleus into membrane-bound vesicles (apoptotic bodies) were also observed (Fig. 3C).

Furanodiene-induced apoptosis was further investigated using agarose gel electrophoresis of the DNA degraded by internucleosomal DNA fragmentation. The treatment of MCF-7 cells with 75 μM and 100 μM furanodiene for 24 h induced a dose-dependent DNA fragmentation, exhibiting a typical DNA ladder feature that could be inhibited by the z-VAD-fmk pretreatment (Fig. 3D).

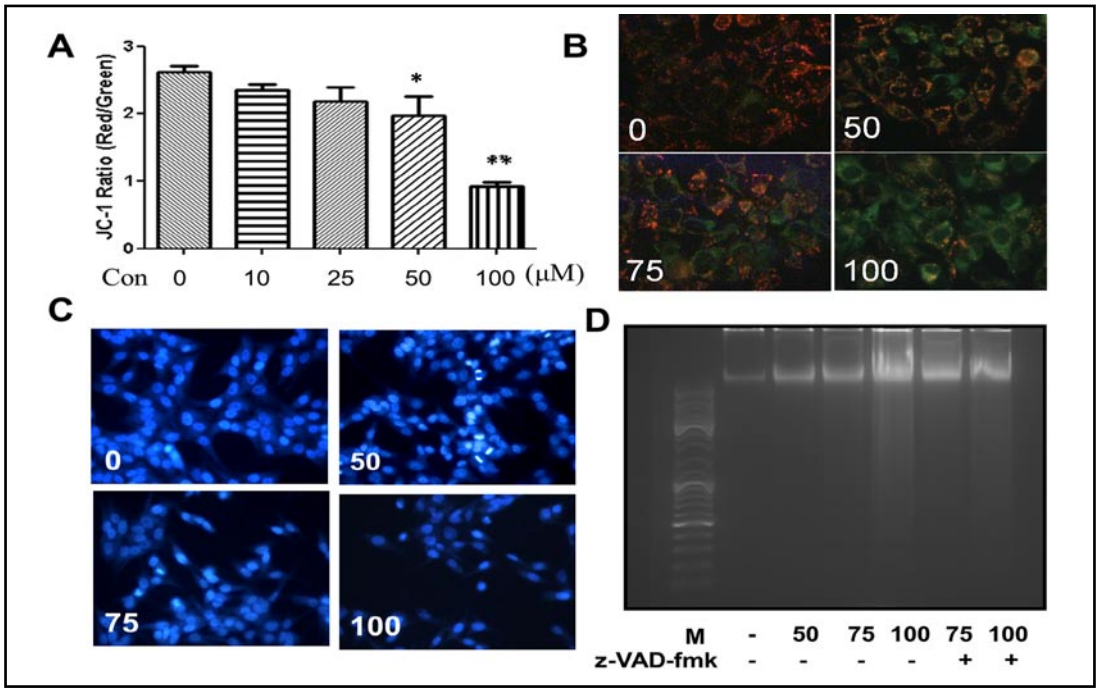

Fig. 3. Effect of furanodiene on ΔΨm and cell apoptosis in breast cancer line cells. MDA-MB-231 and MCF-7 cells were treated with different concentrations of furanodiene for 4 h, after which, the ΔΨm was investigated. The ΔΨm was monitored through JC-1, and the red/green fluorescence ratio was calculated for MDA-MB-231 cells (A) and monitored with fluorescence microscopy for MCF-7 cells (B). MCF-7 cells were stained by Hoechst 33342 and observed under an inverted Axiovert 200 fluorescence microscope (C). The DNA ladder assay was also performed in MCF-7 cells (D). Con, concentration. Data are expressed as mean ± SEM. $^{*}P < 0.05$,$^{**}P < 0.01$ *vs.* control.

Table 1. Effect of furanodiene on cell cycle distribution in MCF-7 cells. Data are expressed as mean ± SD. $^{*}P < 0.05$ *vs.* control and $^{***}P < 0.001$ *vs.* control.

Concentration (μM)	(Percent cell in phase %)			
	Sub-G1	G0/G1	S	G2/M
0	4.56 ± 1.26	68.12 ± 4.32	22.93 ± 4.54	8.94 ± 0.75
Fur 50	6.26 ± 0.84	69.32 ± 4.89	25.85 ± 6.24	4.83 ± 1.36*
Fur 75	27.49 ± 2.07 ***	73.94 ± 4.01	19.80 ± 4.31	6.26 ± 2.69
Fur 100	67.99 ± 3.88 ***	82.81 ± 7.54*	10.37 ± 7.39	6.82 ± 1.24
TAM 7.5	5.97 ± 0.60	74.30 ± 0.84	15.95 ± 0.94	9.75 ± 0.54

Furanodiene regulates the expression of cell cycle- and apoptosis-relevant proteins

Western blotting results showed that furanodiene dose-dependently decreased the protein expression of Rb, cyclin D1, CDK2, integrin β1 (ITG β1), and integrin βV (ITG βV) without affecting the protein expression of p21, Puma, and p53 (Fig. 4, left). Furthermore, furanodiene significantly decreased the protein expression of *p*-cyclin D1 (Thr286), *p*-CDK 2 (Thr160), *p*-Rb (Ser795), and *p*-Rb (Ser807/811) in a dose-dependent manner (Fig. 4, left). In addition, TAM (7.5 μM) treatment decreased the protein expression of *p*-Rb (Ser795), *p*-cyclin D1 (Thr286), *p*-CDK 2 (Thr160), cyclin D1, CDK2, and ITG β1, but failed to regulate the expression of *p*-Rb (Ser807/811), Rb, p21, Puma, p53, and ITG βV (Fig. 4, left).

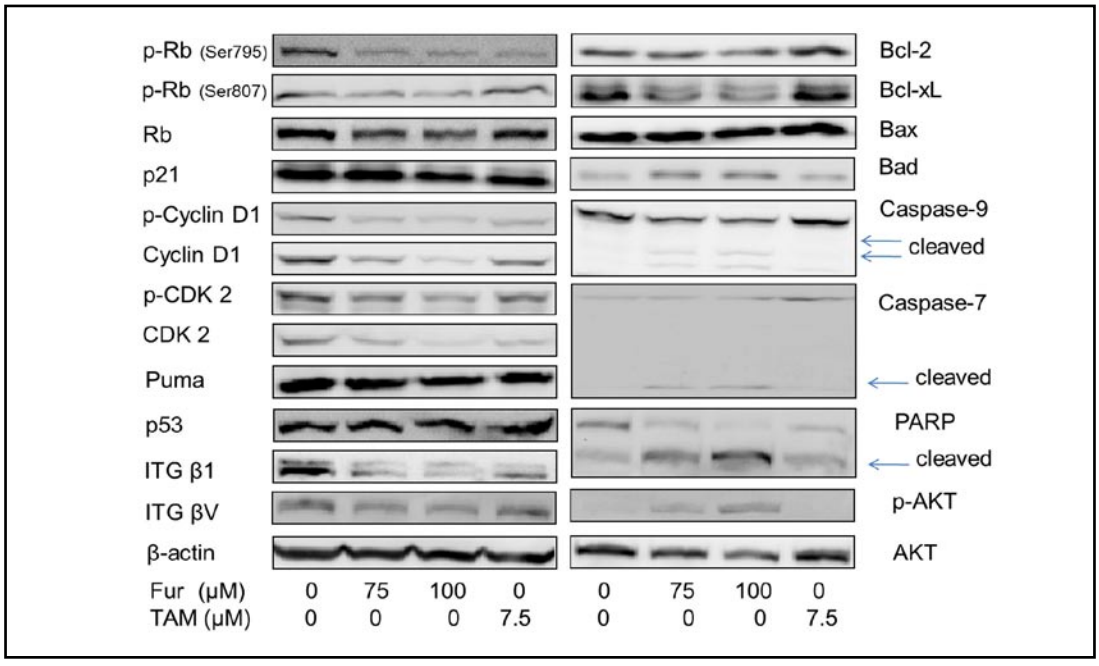

Fig. 4. Effect of furanodiene on cell cycle- and apoptosis-relevant protein expressions in MCF-7 cells. The protein expression was determined by Western blotting. The MCF-7 cells were treated with furanodiene or TAM for 24 h. β-actin was used as a loading control and a relative protein level control. The Western blotting data presented are representative of at least three independent experiments.

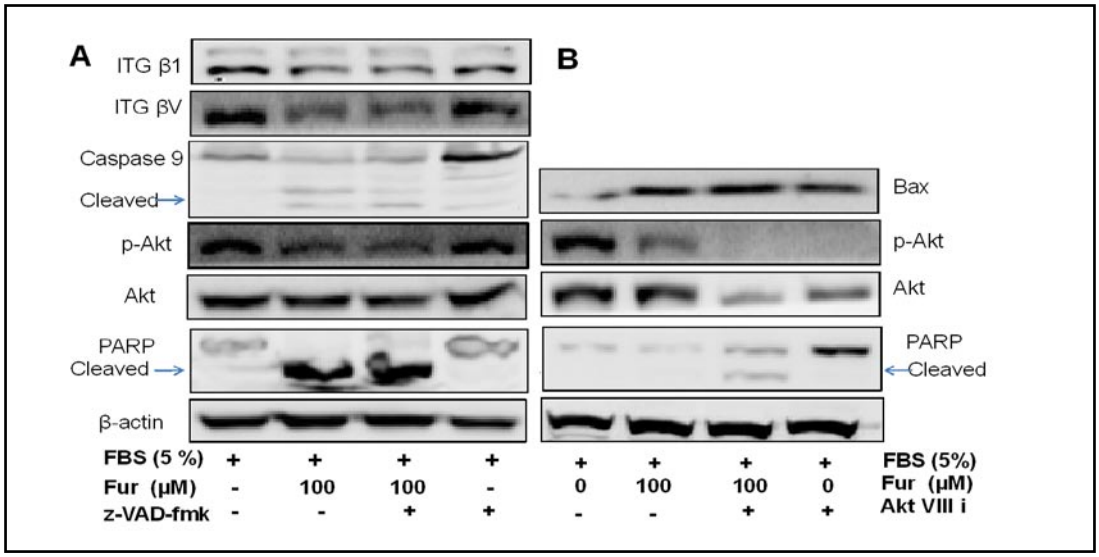

Fig. 5. Effect of z-VAD-fmk or Akt VIII inhibitor on furanodiene-induced apoptotic proteins and Akt and *p*-Akt expressions under high FBS conditions. The MCF-7 cells were pretreated with z-VAD-fmk (A) or Akt VIII inhibitor (B) for 1 h and then treated with furanodiene for 24 h. Whole cell lysates were subjected to SDS-PAGE and Western blot assay.

For the Bcl-2 family members, furanodiene treatment suppressed the protein expression of Bcl-xL, and increased that of Bad without affecting the expressions of Bcl-2 and Bax (Fig. 4, right). Furthermore, furanodiene induced the activation of caspase-9, caspase-7, and PARP in a dose-dependent manner, as indicated by their decreased protein expression (Fig. 4,

Table 2. The anti-tumor effect of furanodiene in nude mice xenografts. $^{**}P < 0.05$ *vs.* control.

Treatment	Weight (g)		Tumor weight (g)	Inhibition (%)
	Beginning	End		
Control	21.43±2.38	21.48±2.72	1.16±0.41	—
CTX (30mg/kg)	21.08±0.96	19.8±0.40	0.48±0.13 **	58.43%
Fur (30mg/kg)	20.67±1.53	20.62±1.65	0.53±0.11**	54.52%
Fur (15mg/kg)	21.47±1.46	21.40±1.64	0.78±0.23	33.19%

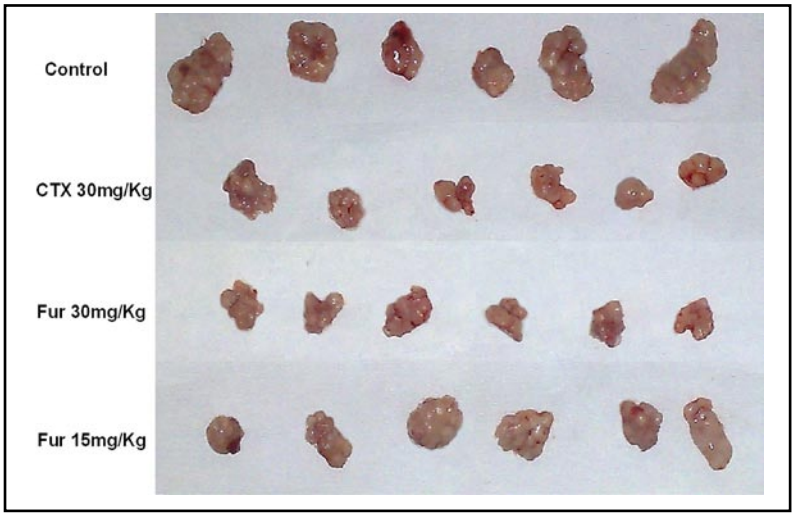

Fig. 6. Effect of furanodiene on breast cancer tumor growth in nude mice xenografts. A nude mice tumor xenograft model was established with MCF-7 cells and treated with furanodiene (15 mg/kg and 30 mg/kg) once daily for 8 days. CTX was used as positive control.

right). The expression ratio of *p*-Akt to Akt was also increased by furanodiene treatment. In TAM-treated cells, the expression of cleaved PARP was increased, whereas the expression of Bcl-2, Bcl-xL, Bax, Bad, caspase-9, caspase-7, *p*-Akt (Ser 473), and Akt was not affected (Fig. 4, right).

Effects of z-VAD-fmk and Akt inhibitor VIII on furanodiene-induced protein expressions

z-VAD-fmk, a cell-permeable pan caspase inhibitor, and the Akt inhibitor VIII, a potent and selective inhibitor of Akt1/2, were pretreated respectively before furanodiene treatment to explore the role of caspases and Akt in furanodiene-induced apoptosis. In 5% FBS, furanodiene induced the proteolytic cleavage of PARP, and decreased the expression of ITG β1, ITG βV, *p*-Akt, and Akt were not affected by z-VAD-fmk pretreatment. However, the proteolytic cleavage of caspase-9 was inhibited (Fig. 5A). The furanodiene-induced decrease of *p*-Akt and Akt expressions was enhanced by the Akt inhibitor VIII pretreatment. Furthermore, the furanodiene -induced PARP cleavage was enhanced by Akt inhibitor VIII pretreatment. The Akt inhibitor VIII showed no effect on cleaved PARP expression but decreased the *p*-Akt and Akt expressions (Fig. 5B).

Furanodiene inhibits growth of breast cancer tumor in nude mice xenografts

An MCF-7 tumor xenograft model was established to determine whether furanodiene exerts anti-tumor effects *in vivo*. Furanodiene and the positive control CTX were administered to mice once daily for 8 days, and the therapeutic effects were evaluated by examining the tumor weight. Compared with the control group, furanodiene significantly inhibited breast tumor growth in a dose-dependent fashion (Fig. 6 and Table 2). The administration at 15 mg/kg and 30 mg/kg doses resulted in 33.19% and 54.52% tumor growth inhibition,

respectively. No significant difference was found between the inhibitory rates of furanodiene and CTX at 30 mg/kg. In addition, the body weights of the mice were unchanged throughout the test duration (Table 2).

Discussion

Previously, both furanodiene and germacrone were identified as the main components in the essential oil of *C. wenyujin* [24]. Recently, germacrone was demonstrated to possess anti-breast cancer properties *in vitro* [23], while furanodiene was discovered to show a greater anti-proliferation effect on breast cancer cells. Therefore, in the present study, the anti-cancer activity of furanodiene was evaluated and its molecular mechanism was explored *in vitro* and *in vivo*.

The IC_{50} for furanodiene on MCF-7 cells was about 75 μM after 72 h treatment, which was much less than that of germacrone [23], suggesting that furanodiene might have more anti-cancer potential compared with germacrone. The furanodiene-induced cytotoxicity could be significantly reversed by caspase inhibitor z-VAD-fmk and enhanced by the Akt inhibitor VIII, suggesting that furanodiene could affect caspases and Akt signaling pathways. Furanodiene showed no cytotoxic effect on MCF-10A non-tumorigenic breast epithelial cells and HL-7702 human liver cells [25] even at 100 μM. The finding suggests a certain selectivity for cancer cells, which was not observed in Dox, the common anti-cancer agent used in the treatment of a number of neoplasms. Similar with germacrone [23], furanodiene dose-dependently increased the LDH release from both MCF-7 and MDA-MB-231 cells but showed greater potency. Given that LDH is a sensitive marker for cell membrane integrity, the large amount of LDH released from both cell lines after furanodiene treatment is an indication of a significant damage. Consolidating all the findings, furanodiene is demonstrated to be clearly cytotoxic to both breast cancer cell lines.

The mitochondria, which are powerhouses of the cells, have been proposed as a potential drug target for cancer therapy [26], mainly because of the mitochondria-mediated apoptosis pathways [27]. The reduction or loss of $\Delta\Psi m$ is an early indicator of apoptosis and a key indicator of cellular viability. The JC-1 staining clearly demonstrated that furanodiene treatment significantly induced breast cancer $\Delta\Psi m$ loss, suggesting that furanodiene induced breast cancer cell apoptosis through mitochondrial-mediated pathways. This finding was further confirmed through Hoechst 33342 staining, the accumulation of the sub-G1 phase, and the DNA ladder assay. Therefore, furanodiene inhibits breast cancer cell proliferation mainly by inducing apoptosis.

The Bcl-2 family proteins are well-known key regulators of apoptosis, which include both the anti-apoptotic proteins such as (Bcl-2, Bcl-xL, Bcl-w, and Boo) and the pro-apoptotic proteins (such as Bax, Bak, Box, Bid, Bim, Bad, and Puma) [28]. A previous study reported that furanodiene showed no effect on Bcl-2, Bax and Bcl-xL protein expressions in HL-60 leukemia cells [16]. In the present study, furanodiene treatment downregulated Bcl-xL and upregulated Bad. However, furanodiene did not affect Bcl-2, Bax and Puma. Thus, different mechanisms might be involved in furanodiene-mediated apoptosis in different cell lines. In addition, furanodiene showed no effect on p53 expression, suggesting that p53 was not involved in this process.

The activation of caspases and PARP cleavage are also important apoptotically relevant events. Caspases involved in apoptosis are generally divided into two categories, namely, the initiator caspases (which include caspase-2, -8, -9, and -10) and the effector caspases (which include caspase-3, -6, and -7) [29]. Caspase-9 plays a central role in the mitochondrial or intrinsic apoptotic pathway by activating caspase-3 and -7, which participate both in intrinsic (mitochondria-mediated) and extrinsic (death receptor-mediated) apoptotic pathways.

Similar to a previous report, furanodiene activated caspase-9 and induced PARP cleavage [16]. The present study also showed that, similar to germacrone [23], furanodiene also activates caspase-7. These results collectively suggest that furanodiene-induced apoptosis in breast cancer cells operated through mitochondria-mediated pathways, similar to the previous report on HepG2 cells [21]. However, further study is needed to elucidate the involvement of TNFR1-mediated extrinsic apoptotic pathways as reported in HL-60 cells [16].

The effect of furanodiene on the cell cycle was not well established. Only the authors' previous study showed that in HepG2 cells, furanodiene induced the G2/M phase arrest. In the present study, furanodiene was found to induce G0/G1 phase arrest. The cell cycle is precisely controlled by a family of proteins called cyclin-dependent kinases (CDKs), which are positively regulated by cyclins (A, B, D, and E) and negatively regulated by cyclin-dependent kinase inhibitors (CDKIs). The G1-phase progression requires the activities of cyclin D-Cdk4/6 complexes, and the G1/S phase transition needs cyclin E-Cdk2 activity. These G1 cyclin-Cdk complexes regulate the cell cycle through the phosphorylation of the retinoblastoma protein (pRb) p107 and pRb family proteins and p130. In the quiescent G0 phase, pRb is nonphosphorylated, whereas in the early G1 phase and late G1 phase, it is sequentially hypophosphorylated and hyperphosphorylated by cyclin D-Cdk4/6 complexes and cyclin E-Cdk2 complex, respectively [30]. Therefore, the reduction of the G1 phase cell cycle-related proteins of *p*-cyclinD1, cyclin D1, *p*-CDK2, CDK2, Rb, and pRb by furanodiene might account for the G0/G1 phase arrest. The p21 protein is a well-known CDKI that inhibits the activity of cyclin-CDK2 or -CDK4 complexes, and thus functions as a regulator of cell cycle progression at G1. In the present study, furanodiene showed no effect on p21 protein expression, which might result from its failure in regulating the p53 expression, since the expression of p21 is tightly controlled by p53 [31].

Akt, a serine/threonine protein kinase, plays an important role in multiple cellular processes such as cell proliferation, cell cycle, apoptosis, transcription, and cell migration. However, the role of Akt in breast cancer cell apoptosis is still under debate [32-34]. Furanodiene increased the expression ratio of *p*-Akt to Aktat Ser 473 under low FBS (0.5%) condition. On the other hand, under high FBS (5%) conditions, furanodiene inhibited Akt phosphorylation, which could not be affected by z-VAD-fmk. Furthermore, furanodiene enhanced the Akt inhibitor-induced decreased expression of Akt and *p*-Akt. These data suggested that the regulation of the Akt pathway might be another underlying mechanism of furanodiene in breast cancer cells.

Finally, a MCF-7 tumor xenograft model was used to confirm the anti-tumor effect of furanodiene *in vivo*. Furanodiene could suppress the growth of breast tumors, and the efficacy is comparable to that of CTX. Further investigation on these results is thus recommended. Furthermore, based on the observation of body weight (Table 2), a small amount of host toxicities were observed after furanodiene treatment.

In conclusion, furanodiene was demonstrated to inhibit breast cancer cell proliferation through apoptosis in a mitochondria-mediated pathway by regulating cyclin D1, CDK2, pRb, and Bcl-2 family proteins, as well as activating caspases and PARP. The Akt pathway might also be involved. Furanodiene also demonstrated anti-tumor effects *in vivo* and could be a lead natural product for further anti-cancer investigation.

Abbreviations

MTT (3-(4,5-dimethylthiazol-2-yl)-2, 5-diphenyltetrazolium bromide); LDH (lactate dehydrogenase); PARP (poly(ADP-ribose) polymerase); US (United States); TNFR1 (tumor necrosis factor receptor 1); MAPK (mitogen-activated protein kinase); FBS (fetal bovine serum); PBS (phosphate-buffered saline); PS (penicillin-streptomycin); PI (propidium iodide); JC-1 (5,5′,6,6′-tetrachloro-1,1′,3,3′-tetraethyl-benzimidazolylcarbocyanine iodide);

PFA (paraformaldehyde); ATCC (American Tissue Culture Collection); EtOH (ethanol); PMSF (phenylmethanesulfonyl fluoride); SDS-PAGE (sodium dodecyl sulfate polyacrylamide gel electrophoresis); PVDF (polyvinylidene fluoride).

Conflict of interest statement

The authors do not have any personal or financial conflict of interest.

Acknowledgements

This study was supported by the Macao Science and Technology Development Fund (Grant nos. 045/2011/A, 077/2011/A3) and the Research Fund of the University of Macau (Grant nos. UL016/09-Y4/CMS/WYT01/ICMS and MYRG208(Y2-L4)-ICMS11-WYT). The authors would like to thank Prof. Shaoping Li (University of Macau, Macau) for providing the furanodiene used in the *in vitro* experiments.

References

1 Efferth T, Li PC, Konkimalla VS, Kaina B: From traditional chinese medicine to rational cancer therapy. Trends Mol Med 2007;13:353-361.
2 Tan W, Lu J, Huang M, Li Y, Chen M, Wu G, Gong J, Zhong Z, Xu Z, Dang Y, Guo J, Chen X, Wang Y: Anti-cancer natural products isolated from chinese medicinal herbs. Chin Med 2011;6:27.
3 Parekh HS, Liu G, Wei MQ: A new dawn for the use of traditional chinese medicine in cancer therapy. Mol Cancer 2009;8:21.
4 Tian G, Guo L, Gao W: Use of compound chinese medicine in the treatment of lung cancer. Curr Drug Discov Technol 2010;7:32-36.
5 Wang S, Penchala S, Prabhu S, Wang J, Huang Y: Molecular basis of traditional chinese medicine in cancer chemoprevention. Curr Drug Discov Technol 2010;7:67-75.
6 Sun Y, Xun K, Wang Y, Chen X: A systematic review of the anticancer properties of berberine, a natural product from chinese herbs. Anticancer Drugs 2009;20:757-769.
7 Epstein J, Sanderson IR, Macdonald TT: Curcumin as a therapeutic agent: The evidence from in vitro, animal and human studies. Br J Nutr 2010;103:1545-1557.
8 Murakami A, Ashida H, Terao J: Multitargeted cancer prevention by quercetin. Cancer Lett 2008;269:315-325.
9 Yao CS: Natural drug: Curcuma wenyujin y.H.Chen et c.Ling. Beijing, People's Health Publishing House, 2008, pp 326.
10 Rui D, Xiaoyan C, Taixiang W, Guanjian L: Elemene for the treatment of lung cancer. Cochrane Database Syst Rev 2007:CD006054.
11 Yang FQ, Li SP, Chen Y, Lao SC, Wang YT, Dong TTX, Tsim KWK: Identification and quantitation of eleven sesquiterpenes in three species of curcuma rhizomes by pressurized liquid extraction and gas chromatography-mass spectrometry. J Pharmaceut Biom Anal 2005;39:552-558.
12 Morikawa T, Matsuda H, Ninomiya K, Yoshikawa M: Medicinal foodstuffs. XXIX. Potent protective effects of sesquiterpenes and curcumin from zedoariae rhizoma on liver injury induced by d-galactosamine/lipopolysaccharide or tumor necrosis factor-alpha. Biol Pharm Bull 2002;25:627-631.
13 Matsuda H, Ninomiya K, Morikawa T, Yoshikawa M: Inhibitory effect and action mechanism of sesquiterpenes from zedoariae rhizoma on d-galactosamine/lipopolysaccharide-induced liver injury. Bioorg Med Chem Lett 1998;8:339-344.
14 Makabe H, Maru N, Kuwabara A, Kamo T, Hirota M: Anti-inflammatory sesquiterpenes from curcuma zedoaria. Nat Prod Res 2006;20:680-685.

15 Sun XY, Zheng YP, Lin DH, Zhang H, Zhao F, Yuan CS: Potential anti-cancer activities of furanodiene, a sesquiterpene from curcuma wenyujin. Am J Chinese Med 2009;37:589-596.
16 Ma E, Wang X, Li Y, Sun X, Tai W, Li T, Guo T: Induction of apoptosis by furanodiene in hl60 leukemia cells through activation of tnfr1 signaling pathway. Cancer Lett 2008;271:158-166.
17 Xiao Y, Yang FQ, Li SP, Gao JL, Hu G, Lao SC, Conceicao EL, Fung KP, Wang YT, Lee SMY: Furanodiene induces g(2)/m cell cycle arrest and apoptosis through mapk signaling and mitochondria-caspase pathway in human hepatocellular carcinoma cells. Cancer Biol Ther 2007;6:1044-1050.
18 Zhong ZF, Hoi PM, Wu GS, Xu ZT, Tan W, Chen XP, Cui L, Wu T, Wang YT: Anti-angiogenic effect of furanodiene on huvecs in vitro and on zebrafish in vivo. J Ethnopharmacol 2012;141:721-729.
19 Wang Y, Liu X, Wang X, Li F, Li J, Cao W: Furanodiene blocks nf-kb-dependent mmp-9 and vegf activation and inhibits cellular invasiveness and angiogenesis of breast cancer cells in vitro and in vivo. Biomedical Research 2012;23:SI 231-237.
20 Chen X, Pei L, Zhong Z, Guo J, Zhang Q, Wang Y: Anti-tumor potential of ethanol extract of curcuma phaeocaulis valeton against breast cancer cells. Phytomedicine 2011;18:1238-1243.
21 Xiao Y, Yang FQ, Li SP, Gao JL, Hu G, Lao SC, Conceicao EL, Fung KP, Wangl YT, Lee SM: Furanodiene induces g2/m cell cycle arrest and apoptosis through mapk signaling and mitochondria-caspase pathway in human hepatocellular carcinoma cells. Cancer Biol Ther 2007;6:1044-1050.
22 Zhong ZF, Li YB, Wang SP, Tan W, Chen XP, Chen MW, Wang YT: Furanodiene enhances tamoxifen-induced growth inhibitory activity of era-positive breast cancer cells in a ppargamma independent manner. J Cell Biochem 2012;113:2643-2651.
23 Zhong Z, Chen X, Tan W, Xu Z, Zhou K, Wu T, Cui L, Wang Y: Germacrone inhibits the proliferation of breast cancer cell lines by inducing cell cycle arrest and promoting apoptosis. Eur J Pharmacol 2011;667:50-55.
24 Yang FQ, Wang YT, Li SP: Simultaneous determination of 11 characteristic components in three species of curcuma rhizomes using pressurized liquid extraction and high-performance liquid chromatography. J Chromatogr A 2006;1134:226-231.
25 Zhang ZY, Pan LJ, Zhang ZM: Functional interactions among stim1, orai1 and trpc1 on the activation of socs in hl-7702 cells. Amino Acids 2010;39:195-204.
26 Armstrong JS: Mitochondria: A target for cancer therapy. Br J Pharmacol 2006;147:239-248.
27 Fulda S: Exploiting mitochondrial apoptosis for the treatment of cancer. Mitochondrion 2010;10:598-603.
28 Ola MS, Nawaz M, Ahsan H: Role of bcl-2 family proteins and caspases in the regulation of apoptosis. Mol Cell Biochem 2011;351:41-58.
29 Shi Y: Mechanisms of caspase activation and inhibition during apoptosis. Mol Cell 2002;9:459-470.
30 Chen CJ, Makino S: Murine coronavirus replication induces cell cycle arrest in g0/g1 phase. J Virol 2004;78:5658-5669.
31 Abbas T, Dutta A: P21 in cancer: Intricate networks and multiple activities. Nat Rev Cancer 2009;9:400-414.
32 Kannaiyan R, Manu KA, Chen L, Li F, Rajendran P, Subramaniam A, Lam P, Kumar AP, Sethi G: Celastrol inhibits tumor cell proliferation and promotes apoptosis through the activation of c-jun n-terminal kinase and suppression of pi3 k/akt signaling pathways. Apoptosis 2011;16:1028-1041.
33 Yuan J, He Z, Wu J, Lin Y, Zhu X: A novel adriamycin analogue derived from marine microbes induces apoptosis by blocking akt activation in human breast cancer cells. Mol Med Report 2011;4:261-265.
34 Chang HL, Sugimoto Y, Liu S, Wang LS, Huang YW, Ye W, Lin YC: Keratinocyte growth factor (kgf) regulates estrogen receptor-alpha (er-alpha) expression and cell apoptosis via phosphatidylinositol 3-kinase (pi3k)/akt pathway in human breast cancer cells. Anticancer Res 2009;29:3195-3205.